Pergamon

Int. J. Heat Mass Transfer. Vol. 41, No. 17, pp. 2677–2685, 1998
© 1998 Elsevier Science Ltd. All rights reserved
Printed in Great Britain
0017-9310/98 $19.00+0.00

PII: S0017-9310(97)00310-4

Numerical solution of boundary layer equations in compressible cross-flow to a cylinder

HALIT KARABULUT
Technical Education Faculty, Gazi University, 06530 Ankara, Turkey

and

Ö. ERCAN ATAER†
Engineering and Architecture Faculty, Gazi University, 06570 Ankara, Turkey

(*Received* 29 *July* 1996 *and in final form* 28 *July* 1997)

Abstract—Two-dimensional, steady-state, compressible boundary layer and energy equations are solved numerically using finite difference method in cylindrical coordinates. The heat transfer from and to an isolated cylinder for cross-flow is calculated up to the separation point iteratively. The velocity and temperature profiles, and local Nusselt numbers around the cylinder are obtained for the constant wall temperature boundary condition at different oncoming velocities. The results are obtained for compressible and incompressible flow and given in diagrams. © 1998 Elsevier Science Ltd. All rights reserved.

INTRODUCTION

The convective heat transfer from and to an isolated cylinder in crossflow is important in many engineering applications. A complicated heat transfer mechanism occurs around the cylinder and the problem has been concerned by a large number of investigators theoretically and experimentally for several physical conditions.

Early works were confined to incompressible adiabatic flows. In most of these studies, the boundary layer equations are solved by transforming to ordinary differential equations using transformations, series and integral methods. Schlichting [1] gives a comprehensive review of these studies. Recent computational approaches may be classified into two groups. In one of these approaches the governing equations are simplified by using additional concepts such as stream function, velocity potential and vorticity. In the other approach the problem is solved in terms of the basic variables; u, v, w and p. When solving the elliptic equations the whole nodal values of variables are simultaneously calculated. Therefore, in solving the complete equations of viscous flow the first approach is preferred, because of less variables and numerous studies have been done to simulate the flow velocity flow fields [2, 3].

When solving boundary layer equations however, which are parabolic, solution is started from one side of solution domain and marched to the other side. The boundary layer equations are mostly solved using the second approach and Shyy [4] gives a review of algorithm used in the second approach.

Beam and Warming [5] presented a method for the numerical solution of the compressible Navier–Stokes equations using an implicit finite-difference, noniterative scheme. Das [6] presented an integral method for computing separated and reattached turbulent boundary layers for incompressible two-dimensional flows. Tchon and Paraschivoio [7], simulated the incompressible flow field around a moving airfoil using a noninertial stream function-vorticity formulation of the two-dimensional, unsteady Navier–Stokes equations. Karniadakis [8] investigated the unsteady forced convective heat transfer from an isolated cylinder in cross-flow for Reynolds numbers up to 200. Using spectral element method and various outflow boundary conditions for the velocity field, results are obtained from the numerical solution of Navier–Stokes and energy equations. Chen and Weng [9] solved the two-dimensional Navier–Stokes and energy equations for both incompressible and compressible flows numerically in the body-fitted coordinates for Reynolds numbers below 40. Results are obtained for the laminar flow over a heated cylinder.

Zukauskas [10] studied the heat transfer of a single tube in cross-flow experimentally in the range of Prandtl number from 0.7–500 and that of Reynolds number from $1–2 \times 10^6$. Tanabe and Kashiwada [11] studied heat transfer from a cylinder in crossflow experimentally for the constant wall temperature and constant heat flux boundary conditions.

The results obtained from the solution of the two-dimensional complete Navier–Stokes equations in the

† Author to whom correspondence should be addressed. Tel.: 00-90-312-2317400. Fax: 00-90-312-2308434. E-mail: ataer@mikasa.mmf.gazi.edu.tr.

NOMENCLATURE

c_p	specific heat at constant pressure [J kg^{-1} K^{-1}]	T_w	cylinder wall temperature [K]
d	tube diameter [m]	u	tangential velocity component [m s^{-1}]
k	thermal conductivity [W m^{-1} K^{-1}]	U_∞	oncoming velocity [m s^{-1}]
Nu	Nusselt number [hd/k]	v	radial velocity component [m s^{-1}].
p	pressure [N m^{-2}]	Greek symbols	
r	radial coordinate [m]	δ	hydrodynamic boundary layer thickness [m]
r_0	cylinder radius [m]	δ_t	thermal boundary layer thickness [m]
R	gas constant [J kg^{-1} K^{-1}]	θ	angular coordinate [rad]
Re	Reynolds number ($U_\infty d/\nu$)	μ	dynamic viscosity [N s m^{-2}]
T	temperature [K]	ν	kinematic viscosity [m^2 s^{-1}]
T_∞	temperature of the oncoming fluid [K]	ρ	density [kg m^{-3}].

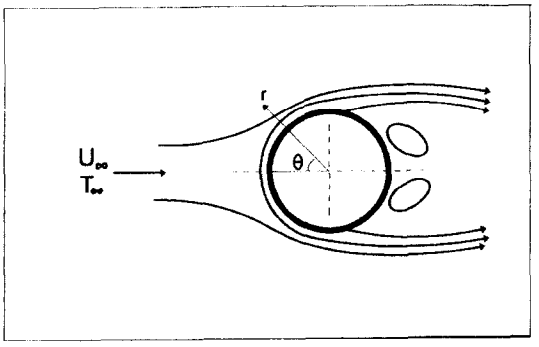

Fig. 1. Physical mechanism and coordinates.

literature are for low Reynolds numbers, because of the complexity of the wake flow behind the tube. At Reynolds number greater than 40 vortex path is formed behind the tube and in some of these studies body-fitted coordinate system is used.

In this study, using finite difference approach two-dimensional boundary layer equations are solved numerically in cylindrical coordinates for compressible cross-flow across an isolated cylinder for different oncoming velocities. The velocity and temperature profiles and the local Nusselt numbers are obtained.

Theory

The physical mechanism and coordinate system is shown in Fig. 1. The predominant velocity component of the flow in the boundary layer is a tangential one. The pressure gradient in the radial direction is negligible in comparison to angular pressure gradient. The angular pressure gradient is known from the inviscid flow analysis initially and there are three unknowns, u, v and T, to be determined by the analysis. The radial component of equation of motion is completely ignored and the unknowns u, v and T are determined by solving the equations of continuity, tangential component of equation of motion and energy equation for compressible flow.

For the compressible flow continuity and the tangential component of the equation of motion are written as, respectively

$$\frac{\partial v}{\partial r}+\frac{v}{r}+\frac{1}{r}\frac{\partial u}{\partial \theta}=-\frac{1}{\rho}\left(v\frac{\partial \rho}{\partial r}+\frac{u}{r}\frac{\partial \rho}{\partial \theta}\right) \tag{1}$$

$$\begin{aligned}\rho\left(v\frac{\partial u}{\partial r}+\frac{u}{r}\frac{\partial u}{\partial \theta}+\frac{vu}{r}\right)&=-\frac{1}{r}\frac{\partial p}{\partial \theta}\\&+\mu\left[\frac{\partial^2 u}{\partial r^2}+\frac{1}{r}\frac{\partial u}{\partial r}-\frac{u}{r^2}+\frac{1}{r^2}\frac{\partial^2 u}{\partial \theta^2}\right.\\&\left.+\frac{2}{r^2}\frac{\partial v}{\partial \theta}+\frac{5}{3r}\frac{\partial}{\partial \theta}\left(\frac{1}{r}\frac{\partial u}{\partial \theta}+\frac{v}{r}+\frac{\partial v}{\partial r}\right)\right]\\&+\frac{\partial \mu}{\partial r}\left(\frac{\partial u}{\partial r}-\frac{u}{r}+\frac{1}{r}\frac{\partial v}{\partial \theta}\right)\\&+\frac{\partial \mu}{\partial \theta}\left(\frac{8}{3r^2}\frac{\partial u}{\partial \theta}+\frac{8v}{3r^2}+\frac{2}{3r}\frac{\partial v}{\partial r}\right)\end{aligned} \tag{2}$$

and the energy equation is written as

$$\begin{aligned}\rho c_p\left(v\frac{\partial T}{\partial r}+\frac{u}{r}\frac{\partial T}{\partial \theta}\right)&=\left[\frac{1}{r}\left(k\frac{\partial T}{\partial r}\right)\right.\\&\left.+\frac{\partial}{\partial r}\left(k\frac{\partial T}{\partial r}\right)+\frac{1}{r^2}\frac{\partial}{\partial \theta}\left(k\frac{\partial T}{\partial \theta}\right)\right]\\&-T\left(\frac{\rho p}{\partial T}\right)\rho\left[\frac{v}{r}+\frac{\partial v}{\partial r}+\frac{1}{r}\frac{\partial u}{\partial \theta}\right].\end{aligned} \tag{3}$$

In the analysis the effects of radiative heat transfer and buoyancy force are ignored. Eliminating density in the above equations using the perfect gas law the eligible form of equations for numerical treatment are stated as follows:

$$\frac{\partial v}{\partial r}+\frac{v}{r}+\frac{1}{r}\frac{\partial u}{\partial \theta}=\left(\frac{v}{T}\frac{\partial T}{\partial r}-\frac{u}{r}\frac{1}{p}\frac{\partial p}{\partial \theta}+\frac{u}{rT}\frac{\partial T}{\partial \theta}\right) \quad (4)$$

$$\left(\frac{pv}{rT}-\frac{\mu}{r}-\frac{\partial \mu}{\partial T}\frac{\partial T}{\partial r}\right)\frac{\partial u}{\partial r}+\left(\frac{pu}{rRT}-\frac{8}{3r^2}\frac{\partial \mu}{\partial T}\frac{\partial T}{\partial \theta}\right)\frac{\partial u}{\partial \theta}+\left(\frac{pv}{rRT}+\frac{\mu}{r^2}+\frac{1}{r}\frac{\partial \mu}{\partial T}\frac{\partial T}{\partial r}\right)u-\left(\frac{2\mu}{r^2}+\frac{1}{r}\frac{\partial \mu}{\partial T}\frac{\partial T}{\partial r}\right)\frac{\partial v}{\partial \theta}-\left(\frac{8}{3r^2}\frac{\partial \mu}{\partial T}\frac{\partial T}{\partial \theta}\right)v-\left(\frac{2}{3r}\frac{\partial \mu}{\partial T}\frac{\partial T}{\partial \theta}\right)\frac{\partial v}{\partial r}-\mu\frac{\partial^2 u}{\partial r^2}-\frac{\mu}{r^2}\frac{\partial^2 u}{\partial \theta^2}=-\frac{1}{r}\frac{\partial p}{\partial \theta}+\frac{5\mu}{3r}\left[\frac{v}{T}\frac{\partial^2 T}{\partial r\,\partial \theta}-\frac{v}{T^2}\frac{\partial T}{\partial \theta}\frac{\partial T}{\partial r}+\frac{1}{T}\frac{\partial v}{\partial \theta}\frac{\partial T}{\partial r}-\frac{u}{rp}\frac{\partial^2 p}{\partial \theta^2}-\frac{1}{rp}\frac{\partial u}{\partial \theta}\frac{\partial p}{\partial \theta}+\frac{u}{rT}\frac{\partial^2 T}{\partial \theta^2}-\frac{u}{rT^2}\left(\frac{\partial T}{\partial \theta}\right)^2+\frac{1}{rT}\frac{\partial u}{\partial \theta}\frac{\partial T}{\partial \theta}+\frac{u}{rp^2}\left(\frac{\partial p}{\partial \theta}\right)^2\right] \quad (5)$$

and

$$\left(\frac{vpc_p}{kRT}-\frac{1}{r}+\frac{vp}{kT}\right)\frac{\partial T}{\partial r}+\left(\frac{upc_p}{rkRT}+\frac{up}{krT}\right)\frac{\partial T}{\partial \theta}-\frac{\partial^2 T}{\partial r^2}-\frac{1}{r^2}\frac{\partial^2 T}{\partial \theta^2}=\frac{1}{k}\left[\frac{\partial T}{\partial r}\frac{\partial k}{\partial T}\frac{\partial T}{\partial r}+\frac{1}{r^2}\frac{\partial T}{\partial \theta}\frac{\partial k}{\partial T}\frac{\partial T}{\partial \theta}\right]+\frac{u}{kr}\frac{\partial p}{\partial \theta}. \quad (6)$$

In the momentum equation $\partial^2 u/\partial\theta^2$ is not ignored because it has the effect of stabilizing the flow about separation point, and the radial pressure gradient $\partial p/\partial r$ and $\partial^2 T/\partial\theta^2$ are ignored. The boundary conditions are written as

$$u=0,\quad \frac{\partial^2 u}{\partial \theta^2}=0,\quad \frac{\partial v}{\partial \theta}=0,\quad \frac{\partial T}{\partial \theta}=0 \quad \text{at } \theta=0 \quad (7a,b,c,d)$$

$$u=0,\quad v=0,\quad T=T_w \quad \text{at } r=0 \quad (8a,b,c)$$

$$u=2U_\infty \sin\theta,\quad T=T_\infty \quad \text{at } r=r_0+\delta. \quad (8d,e)$$

Because of the viscosity of real fluids, on the front of the cylinder a laminar boundary layer develops and its thickness increases downstream. It is assumed that the heat conduction in the flow direction is negligible. The boundary layer equations are simplified by eliminating density assuming that the air is an ideal gas.

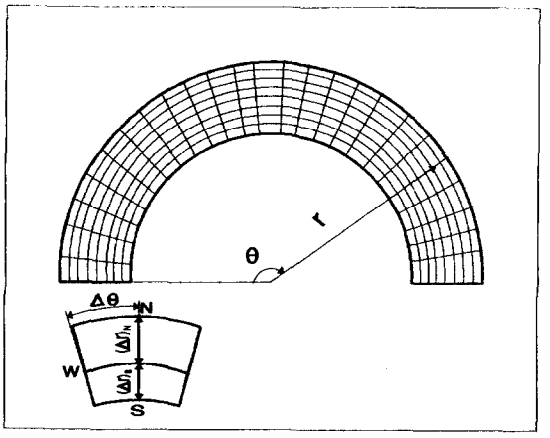

Fig. 2. Discretization of solution domain.

NUMERICAL METHOD

The solution domain used in the analysis is shown in Fig. 2. Considering an element and using the Taylor series expansion values of u and v at the central node are linked to the nodes at the boundary of the element as follows:

$$u-\frac{\partial u}{\partial \theta}\Delta\theta+\frac{\partial^2 u}{\partial \theta^2}\frac{(\Delta\theta)^2}{2}=u_w \quad (9)$$

$$\frac{\partial u}{\partial \theta}-\frac{\partial^2 u}{\partial \theta^2}\Delta\theta=\left(\frac{\partial u}{\partial \theta}\right)_w \quad (10)$$

$$u+\frac{\partial u}{\partial r}(\Delta r)_N+\frac{\partial^2 u}{\partial r^2}\frac{(\Delta r)_N^2}{2}=u_N \quad (11)$$

$$u-\frac{\partial u}{\partial r}(\Delta r)_s+\frac{\partial^2 u}{\partial r^2}\frac{(\Delta r)_s^2}{2}=u_s \quad (12)$$

$$v-\frac{\partial v}{\partial \theta}\Delta\theta=v_w \quad (13)$$

$$v-\frac{\partial v}{\partial r}(\Delta r)_s=v_s. \quad (14)$$

Equations (4), (5) and (9)–(14) are written in matrix form for numerical solution as follows:

$$\begin{bmatrix} K_3 & -K_5 & K_1 & K_2 & -K_6 & K_4 & -\mu & -K_7 \\ 0 & 1/r & 0 & 1/r & 1 & 0 & 0 & 0 \\ 1 & 0 & 0 & -\Delta\theta & 0 & 0 & 0 & \Delta\theta^2/2 \\ 0 & 0 & 0 & 1 & 0 & 0 & 0 & -\Delta\theta \\ 1 & 0 & (\Delta r)_N & 0 & 0 & 0 & (\Delta r)_N^2/2 & 0 \\ 1 & 0 & -(\Delta r)_s & 0 & 0 & 0 & (\Delta r)_s^2/2 & 0 \\ 0 & 1 & 0 & 0 & 0 & -\Delta\theta & 0 & 0 \\ 0 & 1 & 0 & 0 & -(\Delta r)_s & 0 & 0 & 0 \end{bmatrix}$$

$$\begin{bmatrix} u \\ v \\ \partial u/\partial r \\ \partial u/\partial \theta \\ \partial v/\partial r \\ \partial v/\partial \theta \\ \partial^2 u/\partial r^2 \\ \partial^2 u/\partial \theta^2 \end{bmatrix} = \begin{bmatrix} f_1 \\ f_2 \\ u_w \\ (\partial u/\partial \theta)_w \\ u_N \\ u_s \\ v_w \\ v_s \end{bmatrix} \quad (15)$$

$$\begin{bmatrix} 0 & C_1 & -1 & C_2 \\ 1 & (\Delta r)_N & (\Delta r)_N^2/2 & 0 \\ 1 & -(\Delta r)_s & (\Delta r)_s^2/2 & 0 \\ 1 & 0 & 0 & -\Delta\theta \end{bmatrix} \begin{bmatrix} T \\ \partial T/\partial r \\ \partial^2 T/\partial r^2 \\ \partial T/\partial \theta \end{bmatrix} = \begin{bmatrix} f_3 \\ T_N \\ T_s \\ T_w \end{bmatrix} \quad (20)$$

where the values of abbreviated matrix elements are written as:

$$K_1 = \left(\frac{pv}{RT} - \frac{\mu}{r} - \frac{\partial\mu}{\partial T}\frac{\partial T}{\partial r}\right),$$

$$K_2 = \left(\frac{pu}{rRT} - \frac{8}{3r^2}\frac{\partial\mu}{\partial T}\frac{\partial T}{\partial\theta}\right)$$

$$K_3 = \left(\frac{pv}{rRT} + \frac{\mu}{r^2} + \frac{1}{r}\frac{\partial\mu}{\partial T}\frac{\partial T}{\partial r}\right)$$

$$K_4 = \left(\frac{2\mu}{r^2} + \frac{1}{r}\frac{\partial\mu}{\partial T}\frac{\partial T}{\partial r}\right) \quad K_5 = \left(\frac{8}{3r^2}\frac{\partial\mu}{\partial T}\frac{\partial T}{\partial\theta}\right)$$

$$K_6 = \left(\frac{2}{3r}\frac{\partial\mu}{\partial T}\frac{\partial T}{\partial\theta}\right), \quad K_7 = \frac{\mu}{r^2}$$

$$f_1 = -\frac{1}{r}\frac{\partial p}{\partial\theta} + \frac{5\mu}{3r}\left[\frac{v}{T}\frac{\partial^2 T}{\partial r\,\partial\theta} - \frac{v}{T^2}\frac{\partial T}{\partial\theta}\frac{\partial T}{\partial r} + \frac{1}{T}\frac{\partial v}{\partial\theta}\frac{\partial T}{\partial r} - \frac{u}{rp}\frac{\partial^2 p}{\partial\theta^2} - \frac{1}{rp}\frac{\partial u}{\partial\theta}\frac{\partial p}{\partial\theta} + \frac{u}{rT}\frac{\partial^2 T}{\partial\theta^2} - \frac{u}{rT^2}\left(\frac{\partial T}{\partial\theta}\right)^2 + \frac{1}{rT}\frac{\partial u}{\partial\theta}\frac{\partial T}{\partial\theta} + \frac{u}{rp^2}\left(\frac{\partial p}{\partial\theta}\right)^2\right]$$

$$f_2 = \frac{v}{T}\frac{\partial T}{\partial r} - \frac{u}{rp}\frac{\partial p}{\partial\theta} + \frac{u}{rT}\frac{\partial T}{\partial\theta}. \quad (16)$$

The pressure, p in these equations is initially known and taken from the literature [10]. Considering again the element in Fig. 2, the temperature at the central node is linked to the boundary nodes of the element as follows,

$$T + \frac{\partial T}{\partial r}(\Delta r)_N + \frac{\partial^2 T}{\partial r^2}\frac{(\Delta r)_N^2}{2} = T_N \quad (17)$$

$$T - \frac{\partial T}{\partial T}(\Delta r)_s + \frac{\partial^2 T}{\partial r^2}\frac{(\Delta r)_s^2}{2} = T_s \quad (18)$$

$$T - \frac{\partial T}{\partial\theta}\Delta\theta = T_w. \quad (19)$$

Equations (6) and (17)–(19) are written in the matrix form as

where the following abbreviations are used:

$$C_1 = \left(\frac{vpc_p}{kRT} - \frac{1}{r} + \frac{vp}{kT}\right), \quad C_2 = \left(\frac{upc_p}{rkRT} + \frac{up}{krT}\right)$$

$$f_3 = \frac{1}{k}\left[\frac{\partial T}{\partial r}\frac{\partial k}{\partial T}\frac{\partial T}{\partial r} + \frac{1}{r^2}\frac{\partial T}{\partial\theta}\frac{\partial k}{\partial T}\frac{\partial T}{\partial\theta}\right] + \frac{u}{kr}\frac{\partial p}{\partial\theta}. \quad (21)$$

When the matrix equations (15) and (20) are solved for u, v and T, the discretized equations are obtained for numerical solution. Since the algebraic operations are tedious, u, v and T are directly calculated from equations (15) and (20) node by node using a matrix solver.

Numerical operation is started from the stagnation point and marched downward. Depending on the oncoming velocity the appropriate step size in radial direction is determined by trial-and-error method. On the other hand, since the thickness of both the boundary layers initially are not known, the radial dimension of solution domain is determined iteratively. The dimension that satisfies $\partial u/\partial r = 0$ and $\partial T/\partial r = 0$ at infinite is assumed to be appropriate.

This matrix scheme has the following advantages:

(1) The derivative boundary conditions, related to the first or second derivative, are easily satisfied.
(2) If it is needed, in r-direction non-uniform grid dimensions can be introduced for stability. This may be done by setting $(\Delta r)_s = (\Delta r)_N/2$ or $(\Delta r)_N = (\Delta r)_s/2$. When this type of grid dimensions are introduced the boundary values of the grid become $u_s = \frac{1}{2}(u_{i,j} + u_{i,j-1})$, $u_N = \frac{1}{2}(u_{i,j} + u_{i,j+1})$, $v_s = \frac{1}{2}(v_{i,j} + v_{i,j-1})$, etc.

RESULTS

A thin tube with 10 mm diameter in cross flow of air is considered. Calculations are made for two different cases: at first case the surface temperature of the tube is taken as 300 K as free stream temperature is 900 K. In second case the tube temperature is assumed 900 K while the temperature of the free stream is 300 K. The physical properties of the air are taken as a function of temperature and the related correlation are used in calculations.

From the numerical solution of boundary layer and energy equations velocity, temperature fields and the local Nusselt numbers around the cylinder are

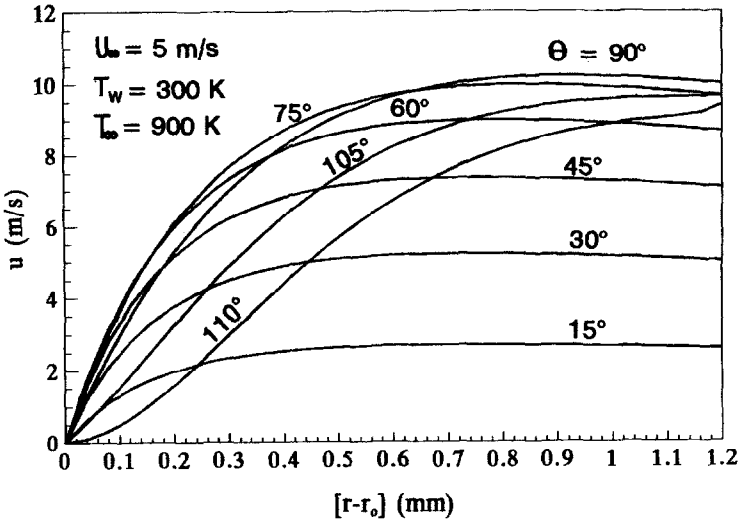

Fig. 3. Profiles of u component of velocity.

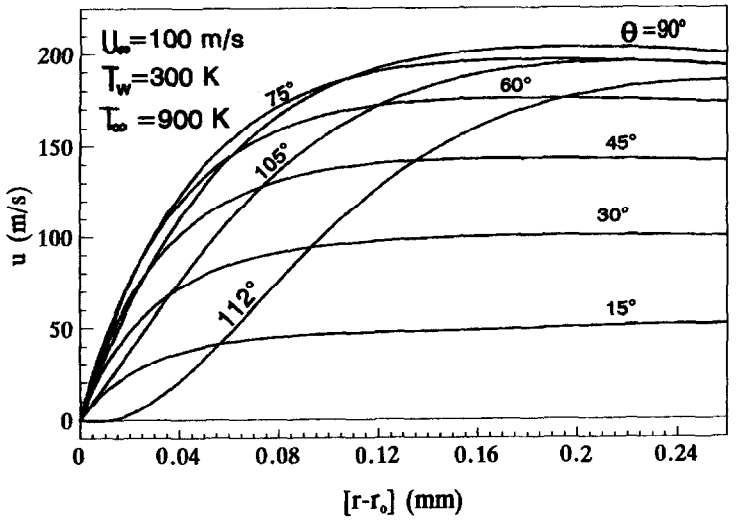

Fig. 4. Profiles of u component of velocity.

obtained up to separation point. The tangential velocity profiles in the boundary layer for different angular positions are shown in Fig. 3 for 5 m s^{-1} oncoming flow velocity. For the oncoming velocity of 100 m s^{-1} the tangential velocity profiles at different angular positions are also given in Fig. 4. For the oncoming flow velocity of 5 m s^{-1} the radial velocity profiles at different angular positions are shown in Fig. 5. The temperature profiles at different angular positions around the cylinder for 5 m s^{-1} oncoming flow velocity are given in Fig. 6 and for 100 m s^{-1} are in Fig. 7. The local Nusselt numbers around the cylinder are given in Fig. 8 for different oncoming velocities.

In the second case the heat transfer from the cylinder to the fluid is calculated for the surface temperature of 900 K and free stream temperature of 300 K. For this case the variation of local heat transfer coefficients with angular position at different oncoming velocities are obtained and given in Fig. 9. For comparison, evaluating the physical properties at film temperature, the local Nusselt numbers for incompressible flow are also obtained and given in Fig. 10.

The thickness of thermal boundary layer is higher than the hydrodynamic boundary layer. Therefore, δ_t is chosen as a criteria to compare with r to show how important the use of cylindrical form of equations. For case one the ratio of δ_t/r is approximately 0.05 which is significant at 100 m s^{-1} oncoming flow velocity. On the other hand, for 5 m s^{-1} oncoming flow velocity this ratio is about 0.20 which shows that at low oncoming flow velocities and small pipe radius it is worthy to use the cylindrical form of boundary layer equations to obtain precise results.

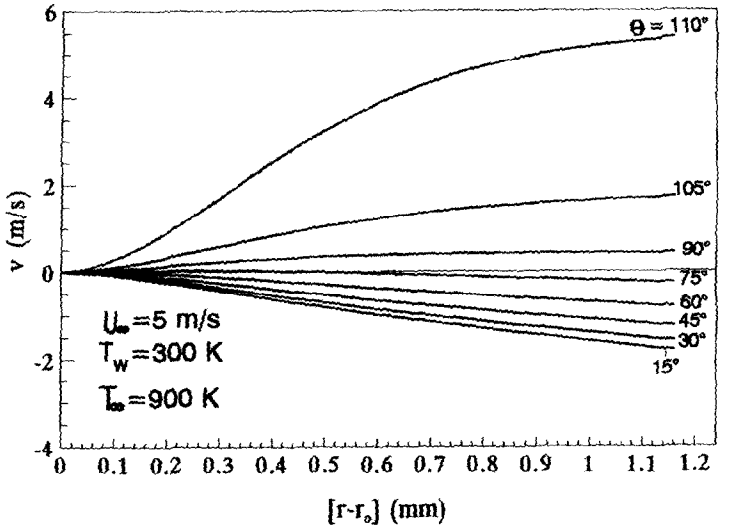

Fig. 5. Profiles of u component of velocity.

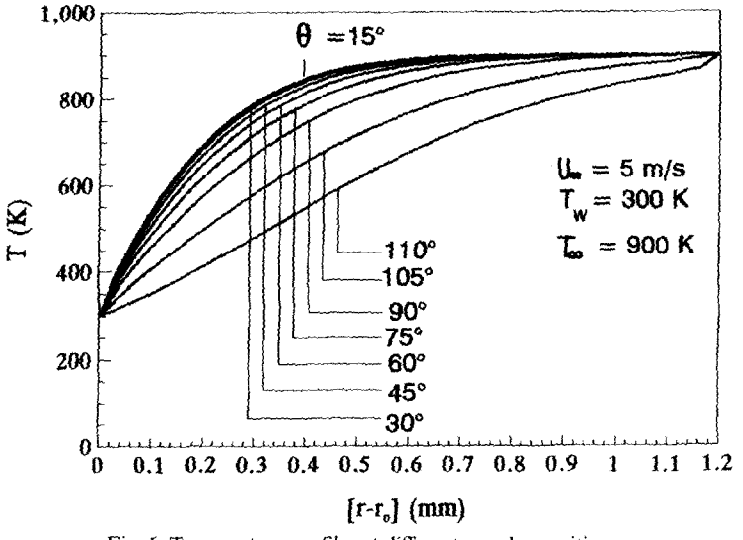

Fig. 6. Temperature profiles at different angular positions.

Heat transfer is considerably influenced by the flow conditions around the cylinder. The local Nusselt number has highest value at stagnation point and decreases by angular position up to separation point as shown in Figs. 8–10.

At low values of temperature difference between the free stream and surface temperature it is found that the results obtained from this analysis are in agreement with the experimental results given in the literature [10]. For the oncoming velocities of 33 m s^{-1} and 155 m s^{-1} which corresponds to Re of 21 000 and 99 000, respectively, and the temperature difference of 100 K the theoretical results are obtained and compared with experimental data in Fig. 11. Slight deviation of the results at high Reynolds numbers are due to the effects of turbulence which is not considered in this study.

In the case of high wall temperature separation of boundary layer takes place at lower angular positions and about 99° within the oncoming velocity range studied.

For case one separation of boundary layer takes place about 110°. It is possible to determine the exact locations with smaller angular step sizes.

The effect of second order angular derivative of tangential velocity, $\partial^2 u/\partial\theta^2$, was investigated and it is found that it has a minor delaying effect on the location of separation point either the flow is compressible or incompressible.

Before 90° the velocity profiles are consistent with

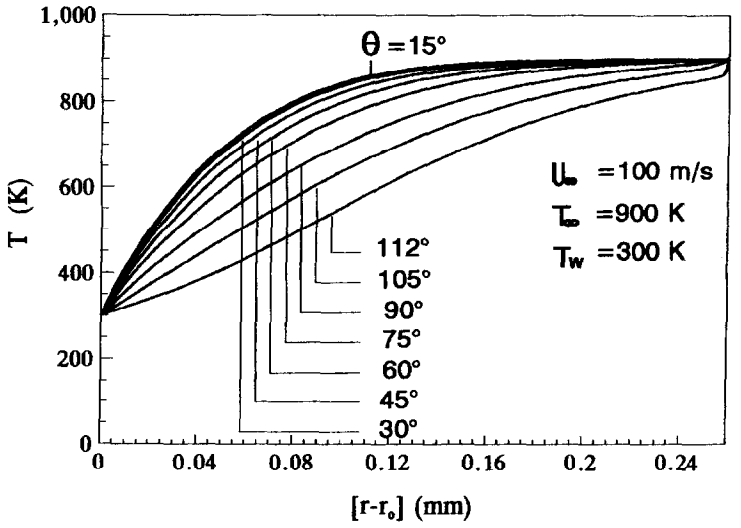

Fig. 7. Temperature profiles at different angular positions.

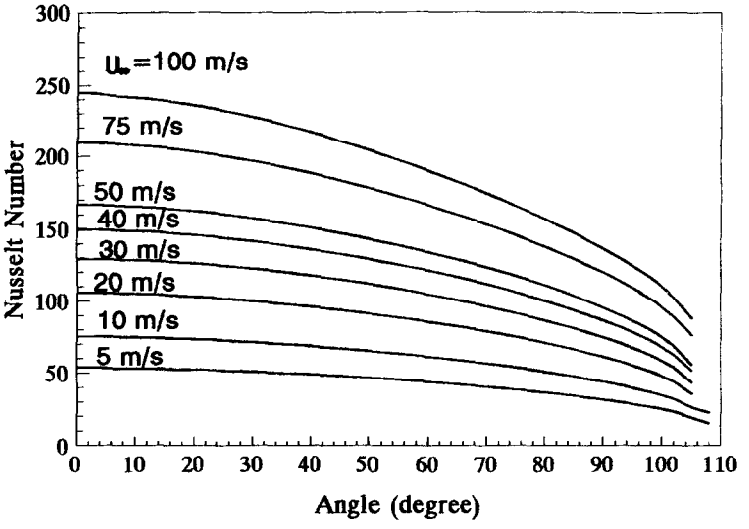

Fig. 8. Nusselt number (T_w = 300 K, T_∞ = 900 K).

boundary layer concept. After 90° the consistency deteriorates gradually and the profile at the separation point is completely inconsistent with the concept. The same tendency is displayed by the temperature profiles.

The radiative heat transfer is ignored in the analysis and it may be considered separately at high surface temperatures. The effect of buoyancy force is also ignored, but its effect may be significant when its direction is the same with the pressure gradient at high surface temperatures.

CONCLUSIONS

Results show that at high temperature differences between free stream flow and surface temperature it is necessary to consider the compressibility of the fluid in the analysis.

As indicated above the result of this study is in agreement with the experimental results. Therefore, the results obtained from this analysis can be used satisfactorily in the practical applications either the experimental data is available or not.

The local Nusselt number is considerably different for cooling and heating of the tube due to the compressibility and changes in physical properties of fluid with temperature.

This matrix scheme has the advantages such as using less grid number by introducing non-uniform grid dimensions, satisfying the derivative boundary conditions easily and avoiding tedious algebraic operations.

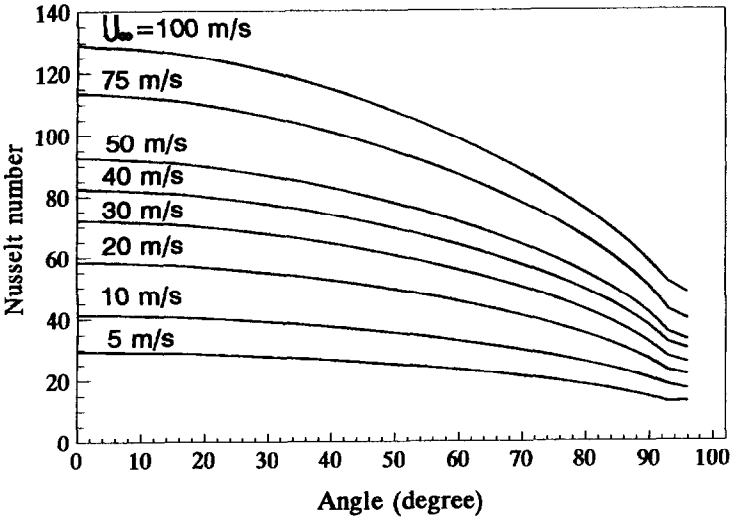

Fig. 9. Nusselt number (T_w = 900 K, T_∞ = 300 K).

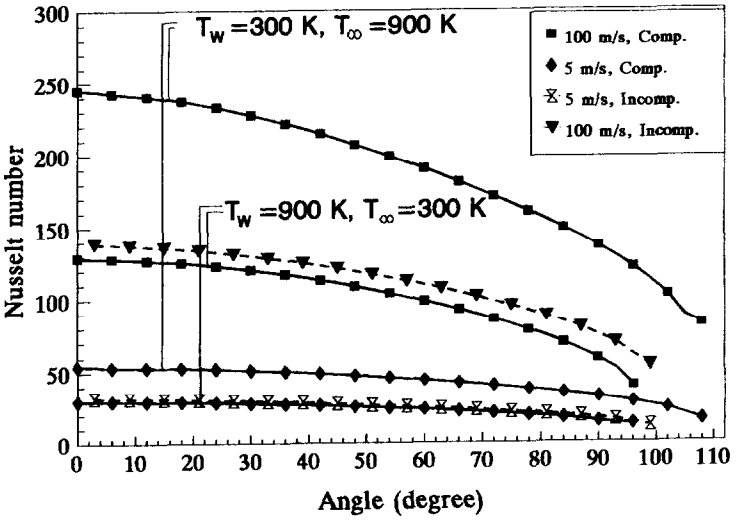

Fig. 10. Comparison of compressible and incompressible treatments.

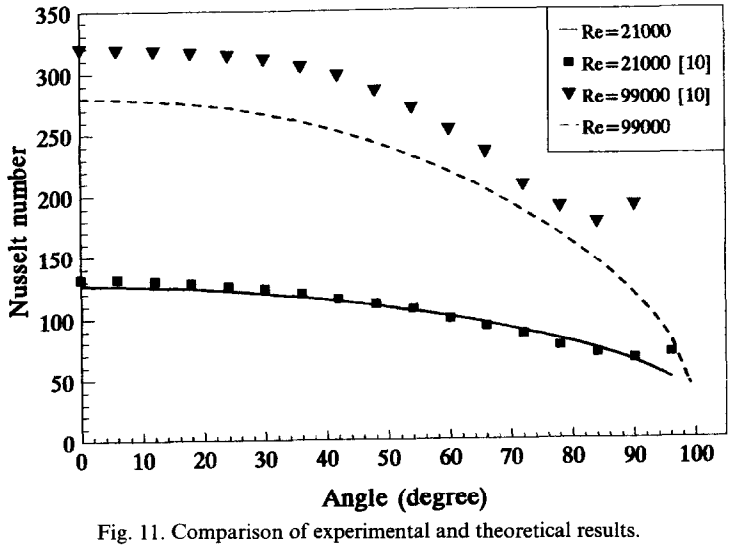

Fig. 11. Comparison of experimental and theoretical results.

REFERENCES

1. Schlichting, H., *Boundary-Layer Theory*. McGraw-Hill Company, 1979.
2. Patankar, S. V. and Spalding, D. B., A finite-difference procedure for solving the equations of the two-dimensional boundary layer. *International Journal of Heat and Mass Transfer*, 1967, **10**, 1389–1411.
3. Patankar, S. V. and Spalding, D. B., Calculation procedure for heat, mass and momentum transfer in three-dimensional parabolic flows. *International Journal of Heat and Mass Transfer*, 1972, **15**, 1787–1806.
4. Shyy, W., Elements of pressure-based computational algorithms for complex fluid flow and heat transfer. *Advances in Heat Transfer*, 1994, **24**, 191–275.
5. Beam, R. M. and Warming, R. F., An implicit factored scheme for the compressible Navier–Stokes equations. *AIAA Journal*, 1978, **16**(4), 393–402.
6. Das, D. K., An inverse inner-variable theory for separated turbulent boundary layers. *Journal of Fluid Engineering*, 1992, **114**, 543–553.
7. Tchon, K. and Patraschivoio, I., Navier–Stokes simulation of the flow around an airfoil in Darrieus motion. *Transactions of the ASME*, 1994, **116**, 870–876.
8. Karniadakis, G. E., Numerical simulation of forced convection heat transfer from a cylinder in crossflow. *International Journal of Heat and Mass Transfer*, 1988, **31**(1), 107–118.
9. Chen, C. and Weng, F., Heat transfer for incompressible and compressible fluid flows over a heated cylinder. *Numerical Heat Transfer, Part A*, 1990, **18**, 325–342.
10. Zukauskas, A., Heat transfer from tubes in crossflow. *Advances in Heat Transfer*, 1987, **18**, 87–159.
11. Tanabe, S. and Kashiwada, Y., Effects of wall boundary layer on local heat transfer from a circular cylinder in cross flow. *Heat Transfer—Japanese Research*, 1993, **22**(5), 506–517.